Effect of the oxidation state of LiNbO₃:Fe on the diffraction efficiency of multiple holograms

Geoffrey W. Burr* and Demetri Psaltis

Department of Electrical Engineering, California Institute of Technology, Pasadena, California 91125

We show that the oxidation state of Fe in LiNbO₃ has two competing effects on the diffraction efficiency of multiple holograms in 90°-geometry holographic storage. For crystals with moderate absorption, the saturation space-charge field is larger after high-temperature reduction treatment. However, reduction also increases absorption, which reduces the overall diffraction efficiency. We develop a theoretical model that predicts achievable diffraction efficiency as a function of oxidation state, doping level, photovoltaic field, crystal length, and region of beam overlap. We compare this model with experimental results for achievable diffraction efficiency and erasure-time constant.   © 1996 Optical Society of America

We analyze here the diffraction efficiency that can be obtained when holograms are angle multiplexed in the 90° geometry shown in Fig. 1. This configuration is attractive for large-scale memories,[1] because it has optimum cross-talk and selectivity characteristics.[2] In this configuration, the reference and the signal beams enter orthogonal crystal faces. A photorefractive crystal is typically used to store the resulting interference pattern. For short exposures, the local permittivity modulation $\Delta\epsilon$ of the recorded hologram depends on the local beam intensities of the two beams and the properties of the crystal. The externally observed diffraction efficiency is the volume integral of this local index modulation weighted by the absorption loss experienced by the readout and diffracted beams. Multiple holograms of equal diffraction efficiency can be stored by use of a recording schedule.[3] For a large number of holograms M, the diffraction efficiency falls as the number of holograms is squared, $\eta = (\mathrm{M}/\#/M)^2$, where $\mathrm{M}/\# = A_0/\tau_r\tau_e$. M/# is a measure of the asymmetry between the writing slope $A_0/\tau_r{}^{\mathrm{ext}}$ and the erasure time $\tau_e{}^{\mathrm{ext}}$. It can be conveniently measured from the growth and decay of a single hologram.[4]

We can maximize M/# by selecting the configuration of the recording beams and the properties of the material. In this Letter we focus on the oxidation state of the photorefractive crystal. Specifically, we consider Fe-doped LiNbO₃, in which Fe^{2+} and Fe^{3+} serve as photon absorber and electron trap, respectively. We can control the ratio of Fe^{2+} to Fe^{3+} densities, and thus the recording and erasure characteristics, by altering the oxidation state of the Fe impurities in the crystal.[5] The optical absorption at a wavelength of ~ 475 nm is a measure of the Fe^{2+} concentrations.[5,6] Our experimental measurements of M/# as a function of the oxidation state in LiNbO₃ show that there is an optimal absorption coefficient. We develop a theoretical model that predicts this optimum.

The experimental measurements were done on a 2 cm × 1 cm × 1 cm LiNbO₃ crystal with 0.01% Fe doping from the Shanghai Institute of Nonmetals. Plane-wave reference and signal beams at 488 nm with equal irradiance were used. A rectangular portion of the recorded grating was sampled by means

of a weak plane-wave readout beam. A_0/τ_r was determined by the slope of $\sqrt{\eta}$ as a function of time. A linear relationship was measured between the writing slope A_0/τ_r and externally measured modulation depth. This implies that the exposure times used (typically $<0.02\ \tau_e{}^{\mathrm{ext}}$) were sufficiently short that the linearized Kukhtarev model would apply.[7] The erasure-time constant was measured after exposure with both the reference and the signal beams. The crystal and the reference beam were rotated by a small angle sufficient for avoiding two-beam coupling during erasure.

After each M/# measurement, the crystal was annealed at 950 °C in an argon–oxygen mixture. A combination of oxygen partial pressure and time was used as the control variable for changing the absorption coefficient. Oxidation was observed to occur more rapidly than reduction. For instance, 30 min of exposure to a 50/50 mixture of argon and oxygen produced a crystal with an absorption coefficient of 0.08 cm⁻¹. Annealing for 3 h in 99.999% pure argon produced a crystal with an absorption of 1.2 cm⁻¹. Absorption was measured at 488 nm in incoherent ordinarily polarized light. No spatial variations in absorption coefficient were observed. For reduction treatments longer than 12 h, the crystal exhibited a small, irreversible absorption increase. Similar "useless" absorption previously observed[5] was attributed to reduction from Nb^{5+} to Nb^{4+}. In Fig. 2 we plot the measured M/# [obtained by multiplying the measured values of $(A_0/\tau_r)^{\mathrm{ext}}$ and $\tau_e{}^{\mathrm{ext}}$] as a function of the absorption coefficient. We have observed the same general dependence of M/# with the absorption coefficient in three other 90°-geometry 0.01% Fe-doped crystals.
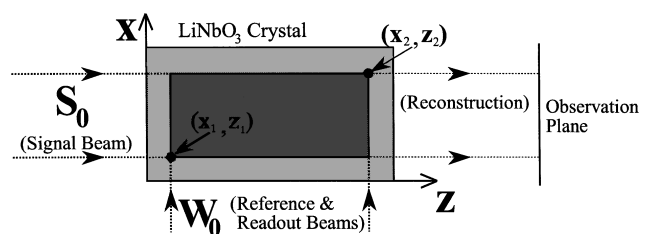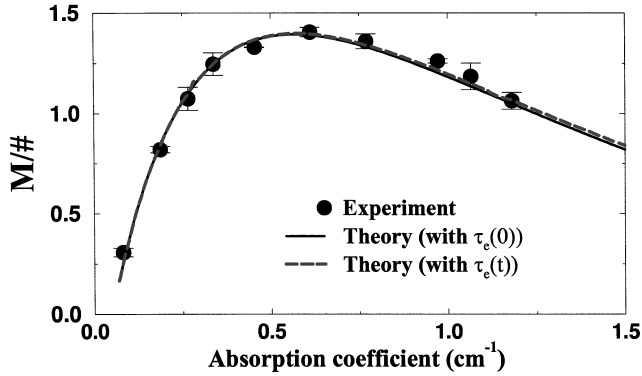

Fig. 1.   90° geometry.

Fig. 2. Dependence of M/# on crystal absorption: solid curve, approximate theory; dashed curve, exact theory.

Also plotted in Fig. 2 is the theoretical prediction for M/#. Our model calculates $(A_0/\tau_r)^{ext}$ and τ_e^{ext}, the two experimentally measured variables that one needs to calculate M#. In each case we evaluate the internal, localized value of the variable. We obtain the external version of these two variables by integrating over the volume of the hologram, using the Born approximation for weak Bragg-matched holograms. The oxidation state affects the externally observed diffraction efficiency through both the photorefractive recording behavior and the bulk absorption of the crystal. The connection between these two is the linear relationship between absorption coefficient and Fe^{2+} concentration.

The initial evolution of the local space-charge field can be obtained from the Kuktarev equation.[7] We follow the analysis in Ref. 8, which introduces a photovoltaic current proportional to the local absorber concentration $[J_{ph} = p(N_D - N_D^+)I]$ and shows that the first-order space-charge field evolves as $E_1(x, z) = m(x, z)E_{sc}\{1 - \exp[-t/\tau_l(x, z)] \exp[-j\omega_l(x, z)t]\}$, where

$$m(x, z) = \frac{\{S_0 \exp[-(\alpha/2)z]\}\{W_0 \exp[-(\alpha/2)x]\}}{I_0(x, z)}, \quad (1)$$

$$E_{sc} = E_q \left[\frac{E_{0ph}^2 + E_D{}^2}{[(N_A/N_D)E_{0ph}]^2 + (E_D + E_q)^2} \right]^{1/2}, \quad (2)$$

$$\tau_l(x, z) = \tau_{di}(x, z)\frac{1 + (E_D/E_\mu)}{1 + (E_D/E_q)} = \frac{\tau_x}{I_0(x, z)}, \quad (3)$$

$$\omega_l(x, z) = \frac{1}{\tau_{di}(x, z)} \frac{N_A E_{0ph}}{N_D E_q} \frac{1}{1 + (E_D/E_\mu)}, \quad (4)$$

and the parameters N_D, N_A, τ_{di}, E_D, E_q, E_μ, and E_{0ph} are defined in Table 1. S_0 and W_0 are the signal and the reference amplitudes, respectively, $I_0(x, z)$ is the local intensity, and α is the intensity absorption coefficient. The annealing process changes the occupancy of the N_A level through the diffusion of oxygen into or out of the crystal. This change of oxidation state affects terms containing N_A or the absorption coefficient α (proportional to $N_D - N_A$), and the total Fe doping N_D remains unchanged during annealing.

Using Eqs. (1)–(4), we can evaluate A_0/τ_r and τ_e locally. For exposure times much shorter than τ_l, the local writing slope is $m(x, z)E_{sc}/\tau_{l(x,z)}[1 + j\tau_l(x, z)\omega_l(x, z)]$. However, the efficiency of the scattering from each point is reduced by the absorption of the readout beam before diffraction $\{\exp[-(\alpha/2)x]\}$ and of the diffracted beam after diffraction $\{\exp[-(\alpha/2)(L - z)]\}$. The effective writing slope seen by an external observer is then

$$\left(\frac{A_0}{\tau_r}\right)^{ext} = bS_0W_0E_q\frac{(E_{0ph}^2 + E_D^2)^{1/2}}{E_q + E_D} \exp\left(-\frac{\alpha}{2}L\right)$$

$$\times \frac{(z_2 - z_1)}{\tau_x} \frac{\exp(-\alpha x_1) - \exp(-\alpha x_2)}{\alpha}, \quad (5)$$

where x_1, x_2, z_1, and z_2 define the region of the crystal used for recording, L is the total length of the crystal in the z direction (i.e., along the signal path), τ_x was defined in Eq. (3), and b is a scaling factor that converts the $E_{sc}L$ product to $\sqrt{\eta}$ (see Table 1).

On erasure, during either readout or storage of subsequent holograms, the local permittivity evolves as $\exp[-t/\tau_l(x, z)]\exp[-j\omega_l(x, z)t]$. Each grating element is decaying and shifting in phase at a rate

Table 1. List of Parameters Used[a]

Symbol	Variable	Definition	Modeled As	Ref.
N_D	Total Fe doping		0.01% Fe $\rightarrow 1.89 \times 10^{18}$ cm^{-3}	5
N_A	Initial Fe^{3+} concentration		$N_D - 1.51 \times 10^{17}\alpha$	5
τ_{di}	Dielectric relaxation time	$(\epsilon/q\mu)[\gamma_R N_A/sI_0(N_D - N_A)]$	$1.90 N_A/I_0(N_D - N_A)$	9,10
E_D	Diffusion field	$k_B TK/q$	$0.163/\Lambda$	
E_q	Saturation space-charge field	$qN_A(N_D - N_A)/\epsilon K N_D$	$9.6 \times 10^{-9}\Lambda(N_A/N_D)(N_D - N_A)$	
E_μ	Drift field	$\gamma_R N_A/\mu K$	$1.77 \times 10^{-8}N_A\Lambda$	9,10
E_{0ph}	Photovoltaic field	$p\gamma_R N_A/q\mu s$	$(10^{-15} - 3 \times 10^{-14})N_A$	11,12
b	Proportionality constant	$\dfrac{4n_o}{(n_o + 1)^2}\left(\dfrac{2\pi}{\lambda}\right)\dfrac{n_o^3 r_{13}}{[(z_2 - z_1)(x_2 - x_1)]^{1/2}}$	$\dfrac{6.74 \times 10^{-4}}{[(z_2 - z_1)(x_2 - x_1)]^{1/2}}$	

[a]Fields are in terms of volts per centimeter; concentrations are in cubic centimeters. All parameters are functions of α in inverse centimeters, and grating period Λ is in centimeters.

set by the local erasure intensity. As a result, the externally observed decay cannot be described by a single exponential. Intuitively, this is because the local erasure constant is smallest for the grating elements first encountered by the erasing beams. As these sections are quickly erased and contribute less to the diffracted output, the observed decay rate decreases. For moderate absorption coefficients, this effect is negligible over the duration of a standard recording schedule. We show that this is indeed the case for the experiments we have performed.

As a result, we can assume that τ_e^{ext} at time $t = 0$ is an accurate description of the hologram decay during the entire recording schedule. It turns out that the evolution of the grating during erasure can be written as $\sqrt{\eta}(t) \propto \iint \exp(-\alpha x) \exp[-t/\tau_x I_0(x, z)] \mathrm{d}x \mathrm{d}z = \iint \exp(-\alpha x) \exp\{-t/\tau_x [S_0^2 \exp(-\alpha z) + W_0^2 \exp(-\alpha x)]\} \mathrm{d}x \mathrm{d}z$. We solve for the external erasure time constant as follows:

$$\frac{1}{\tau_e^{\text{ext}}\big|_{t=0}} \equiv \frac{\frac{-\mathrm{d}}{\mathrm{d}t}(\sqrt{\eta}|_{t=0})}{\sqrt{\eta}|_{t=0}} = \frac{1}{\tau_x}\left\{\frac{W_0^2}{2}[\exp(-\alpha x_1) + \exp(-\alpha x_2)] + \frac{S_0^2}{\alpha}\frac{\exp(-\alpha z_1) - \exp(-\alpha z_2)}{z_2 - z_1}\right\}. \quad (6)$$

Combining this estimate for τ_e^{ext} with the $(A_0/\tau_r)^{\text{ext}}$ from Eq. (6), we obtain the analytical expression for the effective M/#:

$$\text{M/\#} = b\frac{S_0}{W_0}E_q\frac{(E_{0\text{ph}}^2 + E_D^2)^{1/2}}{E_q + E_D}\frac{\exp\left(-\frac{\alpha}{2}L\right)(z_2 - z_1)[\exp(-\alpha x_1) - \exp(-\alpha x_2)]}{\left(\frac{\alpha}{2}\right)[\exp(-\alpha x_1) + \exp(-\alpha x_2)] + \left(\frac{S_0}{W_0}\right)^2\frac{\exp(-\alpha z_1) - \exp(-\alpha z_2)}{z_2 - z_1}}. \quad (7)$$

The two dominant terms in Eq. (7) are E_q, which increases with absorption (through $N_D - N_A$), and $\exp[-(\alpha/2)L]$, which decreases with absorption. Intuitively, M/# is small for low absorption because the number of photogenerated electrons is small. For higher absorption coefficients, the photorefractive dynamics are no longer absorber limited (but are not yet trap limited). At this point, the losses that are due to bulk absorption rapidly dominate, reducing M/#. Because of the competing effects of bulk absorption and photorefractive dynamics, we expect to find an absorption coefficient that maximizes M/# for any given crystal and geometry.

To predict this maximum accurately, we need the appropriate numerical values. γ_R and s can be determined from photoconductivity measurements and from estimations of the oscillator strength for the Fe^{2+} transition.[5,10] The scaling factor b includes the Fresnel reflection coefficient, electro-optic coefficient, and wavelength, and the beam dimensions needed to convert from output amplitude to $\sqrt{\eta}$. The relationship between absorption and $N_D - N_A$ was discussed in several papers and is quantitatively stated in Ref. 5

for extraordinary absorption at 450 nm. Because we are using ordinary light at 488 nm, a slightly different value gave the best fit to our measured τ_e^{ext} data. The other parameter used for numerically evaluating M/# is $E_{0\text{ph}}$, the photovoltaic field. The value of $1.09 \times 10^{-14}N_A$ that we use for Fig. 2 is in the middle of the wide range of values found in the literature (Table 1). Other parameters used to generate Fig. 2 include $L = 1.91$ cm, $x_1 = z_1 = 0.2$ cm, $x_2 = 0.66$ cm, $z_2 = 1.03$ cm, $\Lambda = 1.47 \times 10^{-5}$ cm, $S_0/W_0 = 1.0$, $W_0^2 = 62.5$ mW/cm^2, and $\alpha_{\text{useless}} = 0.05$ cm^{-1}. Useless absorption created by the excess reduction of Nb^{5+} increases bulk absorption but does not enter into the calculation of N_A. Notice the good agreement between the theoretical prediction (solid curve) and the experimental data points in Fig. 2. The dashed curve was numerically evaluated without the approximation of a single erasure-time constant. The approximate theory deviates only slightly, even for relatively high absorption coefficients.

References

1. F. H. Mok, M. C. Tackitt, and H. M. Stoll, Opt. Lett. **16,** 605 (1991).
2. C. Gu, J. Hong, I. McMichael, R. Saxena, and F. Mok, J. Opt. Soc. Am. A **9,** 1 (1992).
3. D. Psaltis, D. Brady, and K. Wagner, Appl. Opt. **27,** 1752 (1988).
4. F. Mok, G. Burr, and D. Psaltis, Opt. Lett. **21,** 896 (1996).
5. W. Phillips and D. L. Staebler, J. Electron. Mat. **3,** 601 (1974).
6. H. Kurz, E. Kratzig, W. Keune, H. Engelmann, U. Gonser, B. Dischler, and A. Rauber, Appl. Phys. **12,** 355 (1977).
7. N. V. Kukhtarev, V. B. Markov, S. G. Odulov, M. S. Soskin, and V. L. Vinetskii, Ferroelectrics **22,** 949 (1979).
8. C. Gu, J. Hong, H. Li, D. Psaltis, and P. Yeh, J. Appl. Phys. **69,** 1167 (1991).
9. E. Kratzig, Ferroelectrics **21,** 635 (1978).
10. R. A. Rupp, R. Sommerfeldt, K. H. Ringhofer, and E. Kratzig, Appl. Phys. B **51,** 364 (1990).
11. D. L. Staebler, in *Holographic Recording Materials*, H. M. Smith, ed., Vol. 20 of Topics in Applied Physics (Springer-Verlag, Berlin, 1977), pp. 101–132.
12. A. Glass, D. Von der Linde, and T. J. Negram, Appl. Phys. Lett. **25,** 233 (1974).